

cluded that the group as a whole represented $\Lambda K^+ K^-$ events, with negligible contamination from the other two final states, and the events were so assigned. The sample of $\Lambda K^0 \bar{K}^0$ fits presented here represents $\sim 30\%$ of the $\Lambda K \bar{K}$ final state. The group as a whole is consistent with being all $\Lambda K^0 \bar{K}^0$ events, exhibiting properties similar to the sample of $\Lambda K^+ K^-$ events, and they were therefore assigned as such.

³J. Mott, R. Ammar, R. E. P. Davis, W. Kropac, F. Schweingruber, M. Derrick, T. Fields, L. Hyman, J. Loken, and J. Simpson, Phys. Rev. Letters **18**, 355 (1967); J. Mott, Ph.D. thesis, Northwestern University, 1967 (unpublished).

⁴V. E. Barnes, B. B. Culwick, P. Guidoni, G. R. Kalbfleisch, G. W. London, R. B. Palmer, D. Radojicic, D. C. Rahm, R. R. Rau, C. R. Richardson, N. P. Samios, J. R. Smith, B. Goz, N. Horwitz, T. Kikuchi, J. Leitner, and R. Wolfe, Phys. Rev. Letters **15**, 322 (1965).

⁵G. S. Abrams, B. Kehoe, R. G. Glasser, B. Sechi-Zorn, and G. Wolsky, Phys. Rev. Letters **18**, 620 (1967).

⁶Our experimental mass resolution function has a width of ~ 18 MeV for the four-constraint $\Lambda K^+ K^-$ fits and ~ 24 MeV for the one-constraint $\Lambda K^0 \bar{K}^0$ fits. The over-all resolution function for the particular admixture of all kinds of fits present in our sample has a width of ~ 20 MeV.

⁷Sheldon L. Glashow and Robert Socolow, Phys. Rev. Letters **15**, 329 (1965). The partial width predicted for the $K \bar{K}$ decay mode is 31 MeV, but there is also an appreciable contribution (17-MeV partial width) predicted for the $K^* \bar{K} + \bar{K}^* K$ mode. A more recent estimate by M. Goldberg et al., Nuovo Cimento **45A**, 169 (1966), puts this latter partial width at 7 ± 4 MeV. The results are also sensitive to the input value for the width of the A_2 which recently appears to show a complex structure [G. Chikovani et al., Phys. Letters **25B**, 44 (1967)].

⁸Jack L. Uretsky, "On the Bosons of Zero Baryon Number as Bound States of Quark-Antiquark Pairs," in High Energy Theoretical Physics, edited by Hadi Aly (to be published). The total width obtained in this calculation is ~ 35 MeV.

⁹The absence of baryon exchange, pointing to a weak $N \bar{N} \phi$ coupling, as predicted by quark and ω - ϕ mixing models, has already been discussed in Ref. 3.

¹⁰K. Gottfried and J. D. Jackson, Nuovo Cimento **33**, 309 (1964).

¹¹R. H. Dalitz, in Proceedings of the International School of Physics Enrico Fermi, Course XXXIII (Academic Press, Inc., New York, 1966), p. 141.

¹²A satisfactory fit for the spin density matrix elements could also be obtained assuming a spin parity of 1^- for the f^* , but it was discarded on the basis of the $K_1^0 K_1^0$ decay mode observed by Barnes et al., Ref. 4.

MULTICHANNEL PHASE-SHIFT ANALYSIS OF $\bar{K}N$ INTERACTION IN THE REGION 0 TO 550 MeV/c*

Jae Kwan Kim†

Yale University, New Haven, Connecticut

(Received 18 August 1967)

Multichannel phase-shift analysis has been performed on available experimental data for all channels of $K^- p$ and $K_2^0 p$ interactions in the momentum region 0 to 550 MeV/c.¹ In this analysis, the multichannel effective-range parametrization of Ross and Shaw² has been applied. The results on the S_{01} phase shift give the mass and width of the $\bar{K}N$ bound state which are, respectively, lower and larger than the values obtained from the previous constant-scattering-length analysis. The P_{13} phase shift shows that $Y_1^*(1385)$ is due mainly to strong $\Lambda\pi$ interaction and that its coupling to $\bar{K}N$ is very weak. Also in this analysis, the Fermi-Yang ambiguity in $I=0$ $K^+ n$ phase shift of Stenger et al.³ can be resolved and the Yang set is definitely favored.

Available experimental cross sections and angular distributions from approximately 22 000 events of the following ten reactions below 550

MeV/c have been analyzed:

$$\begin{aligned} K^- + p &\rightarrow K^- + p, \\ K^- + p &\rightarrow \bar{K}^0 + n, \\ K^- + p &\rightarrow \Sigma^+ + \pi^-, \\ K^- + p &\rightarrow \Sigma^- + \pi^+, \\ K^- + p &\rightarrow \Sigma^0 + \pi^0, \\ K^- + p &\rightarrow \Lambda + \pi^0, \\ K^- + p &\rightarrow \Lambda + \pi^+ + \pi^-, \\ K_2^0 + p &\rightarrow K_1^0 + p, \\ K_2^0 + p &\rightarrow \Sigma^0 + \pi^+, \\ K_2^0 + p &\rightarrow \Lambda + \pi^+. \end{aligned}$$

The experimental results come mainly from the following three experiments. The cross sections and angular distributions from 0 to

280 MeV/c based on 10 000 events for the first six reactions were analyzed by Kim⁴ in terms of six *s*-wave constant-scattering-length parameters. Watson, Ferro-Luzzi, and Tripp⁵ obtained 10 000 events between 250 and 550 MeV/c for the first seven reactions, and they fitted the results to a constant-scattering-length model using 30 parameters for *s*, *p*, and *d* partial waves. Recently, Kadyk *et al.*⁶ carried out an experiment on $K_2^0 p$ interaction from 100 to 500 MeV/c and obtained approximately 2000 events for the last three reactions. The angular distribution of $K_2^0 p \rightarrow \Lambda \pi^+$ showed that a substantial amount of *p* wave exists even at 160 MeV/c. The detailed angular distributions for $\Lambda \pi^0$ channel were not available prior to this $K_2^0 p$ experiment, because of an experimental difficulty in separating $\Sigma^0 \pi^0$ and $\Lambda \pi^0$ channels. The objective of this work was to make a first over-all coupled-channel phase-shift analysis of the above three experiments using the effective-range parametrization.

Dalitz and Tuan⁷ first formulated the *K*-matrix analysis of $\bar{K}N$ interactions. Ross and Shaw² subsequently gave an effective-range parametrization of the *K* matrix. They defined the *M* matrix and expanded it in the following effective-range form:

$$M(E) = M(E_0) + \frac{1}{2} \delta_{ij} r^{1-2l} C_l (k^2 - k_0^2), \quad (1)$$

where *k* is the diagonal matrix of the center-of-mass channel momenta, *l* is the orbital angular momentum, *r* is the diagonal effective-range matrix, and $C_0 = 1$ for *s* wave and $C_1 = -3$ for *p* wave. They show that off-diagonal ranges are an order of magnitude smaller than the diagonal ranges. This matrix is related to the scattering matrix *T* by

$$T = k^{2l} / (M - ik^{2l+1}). \quad (2)$$

The *M* matrix is essentially the inverse of the *K* matrix, except that the centrifugal barrier factor and the *K* matrix can be calculated from

$$K = k^l M^{-1} k^l. \quad (3)$$

The *I*=0 system has two coupled channels, $\bar{K}N$ and $\Sigma\pi$, whereas the *I*=1 system consists of three coupled two-body channels, $\bar{K}N$, $\Sigma\pi$, and $\Lambda\pi$. From unitarity and time-reversal invariance, both *M* and *K* matrices are real and symmetric. Therefore, we have nine zero-energy parameters and five ranges for each

partial wave. As *s* wave dominates the region below 550 MeV/c, it is possible to determine all 14 parameters for *s* wave within the present statistical accuracy. Present data do not allow the meaningful extraction of effective ranges for P_{01} , P_{11} , and P_{03} partial waves because of the small amount of these waves seen, mainly in the higher half of the energy region investigated. However, effective ranges have been introduced for the P_{13} wave in order to take care of the high-energy tail of $Y_1^*(1385)$ seen in $K_2^0 p - \Lambda \pi^+$ data. The Breit-Wigner resonant amplitude with energy-dependent width⁸ has been used for the D_{03} channel for the $Y_0^*(1520)$, and the presence of a slight amount of D_{13} wave is treated by four constant-scattering-length parameters. Therefore, we used altogether 44 parameters to make the over-all fit of available experimental data.

In the search of these parameters, we used the general minimizing program MINFUN written by Humphrey.⁹ The results of parameters determined in this analysis are given in Table I. The *s*-wave parameters are well determined and are unique. However, only the best parameters with the lowest χ^2 value for higher partial waves have been listed. It is important to point out that these parameters give phase shifts not only for $\bar{K}N \rightarrow \bar{K}N$, but also for $\pi Y \rightarrow \pi Y$ scatterings. This is one of the important features of the *K*-matrix approach.

Figures 1(a)-1(d) present some of the experimental cross sections compared with the calculated values from the fitted parameters. The fit is very good in general, and there are no systematic deviations even at the highest momentum treated in this analysis. It is interesting to point out that there are definite indications of deviations due to the neglect of effective ranges in the separate analyses of the two experiments reported in Refs. 4 and 5. The experimental ratio *R* shown in Fig. 1(e) can be used to solve the Fermi-Yang ambiguity of K^+n phase shifts for the *I*=0 channel from Stenger *et al.*³ The parameters given in Table I combined with the Yang set give good agreement with the data, but the Fermi set can be excluded. This good agreement with the ratio can also be used as a check on the present analysis since the curves shown are not fitted values, but are just predicted values from the parameters. This ratio has been very useful in distinguishing a correct solution from others (as shown by Ref. 6) because the strong

Table I. Multichannel effective-range parameters. M_{AB}^I is the M -matrix element, where I indicates isospin, A and B indicate the initial and the final channel. r_C^I is diagonal range, where I denotes isospin and C denotes channel. M is in units of $F^{-(2I+1)}$ and r is in F . a_1 and b_2 are the real and imaginary parts of the scattering length. ϵ_Σ is the ratio $\sigma(\Sigma\pi)/\{\sigma(\Sigma\pi)+\sigma(\Lambda\pi)\}$, φ_Σ is the phase angle for $KN \rightarrow \Sigma\pi$, and X is the inverse of the interaction radius.

	S	P ₁	P ₃		D ₃	(units)
M_{KK}^0	-0.00±0.02	17.5±16.4	10.9±0.9	a_1	0.006±0.003	(fm ⁵)
$M_{K\Sigma}^0$	-1.11±0.04	-10.6±4.5	-1.4±0.2	b_1	0.002±0.001	(fm ⁵)
$M_{\Sigma\Sigma}^0$	2.04±0.10	-11.4±4.8	5.6±0.5	ϵ_Σ	0.060±0.040	
M_{KK}^1	-3.60±0.02	-18.1±0.7	5.2±1.0	φ_Σ	-4.08±1.50	(rad)
$M_{K\Sigma}^1$	-2.86±0.03	7.2±1.1	-13.8±1.6	E_r	1518.8±0.7	(MeV)
$M_{K\Lambda}^1$	2.08±0.07	4.7±0.4	-11.9±1.6	Γ	16.2±1.0	(MeV)
$M_{\Sigma\Sigma}^1$	-1.40±0.06	-0.3±1.1	-15.8±0.9	Γ_K	5.1±0.4	(MeV)
$M_{\Sigma\Lambda}^1$	1.81±0.04	-6.8±1.0	-13.6±0.2	Γ_Σ	8.8±0.8	(MeV)
$M_{\Lambda\Lambda}^1$	-2.31±0.11	-3.4±1.3	-16.3±2.0	X	0.54±0.05	(fm ⁻¹)
r_K^0	0.54±0.08					
r_Σ^0	-0.89±0.31					
r_K^1	-0.13±0.07		-0.66±0.20			
r_Σ^1	-0.78±0.23		0.27±0.05			
r_Λ^1	-1.22±0.45		0.31±0.13			

$$\chi^2 = 580.0 \text{ for } 565 \text{ degrees of freedom}$$

interference between $S=-1$ and $S=1$ amplitudes appears in a very sensitive manner.

The detailed interpretations of both $Y_0^*(1405)$ and $Y_1^*(1385)$ resonances will be made next using the K -matrix elements obtained for the first time in this analysis. Dalitz¹⁰ defines a resonance energy E_γ for a multichannel system when one of eigenphases passes through a $\frac{1}{2}\pi$ at that energy. The K matrix for πY system below the $\bar{K}N$ threshold is called a reduced K matrix, and it can be expressed in terms of complete K -matrix elements above $\bar{K}N$ threshold in the following form, using Dalitz's notation¹¹:

$$K^R = \gamma - \pi \tilde{\beta} (1 + k\alpha)^{-1} k\beta, \quad (4)$$

where K^R is the reduced K matrix and the eigenvalues of $k^{\frac{1}{2}} K^R k^{\frac{1}{2}}$ give eigenphases $\tan\delta_i$. He classifies resonances into two types: (a) the complete K -matrix elements α , β , and γ may have a pole at the same energy E_γ ; (b) α , β , and γ may vary smoothly, but K^R may have a pole at E_γ when the factor $1 + k\alpha$ becomes zero. The first type is a scattering resonance and the second type is a virtual bound-state resonance. It is shown below that $Y_1^*(1385)$ belongs to the (a) class and $Y_0^*(1405)$ belongs to the (b) class.

In Fig. 2(a), the large value of α indicates that the $\bar{K}N$ channel interaction is strong and the small value of γ shows that the $\pi\Sigma$ channel interaction is weak for the S_{01} system. However, the reduced K matrix $K_{\Sigma\Sigma}^R$ for the $\pi\Sigma$

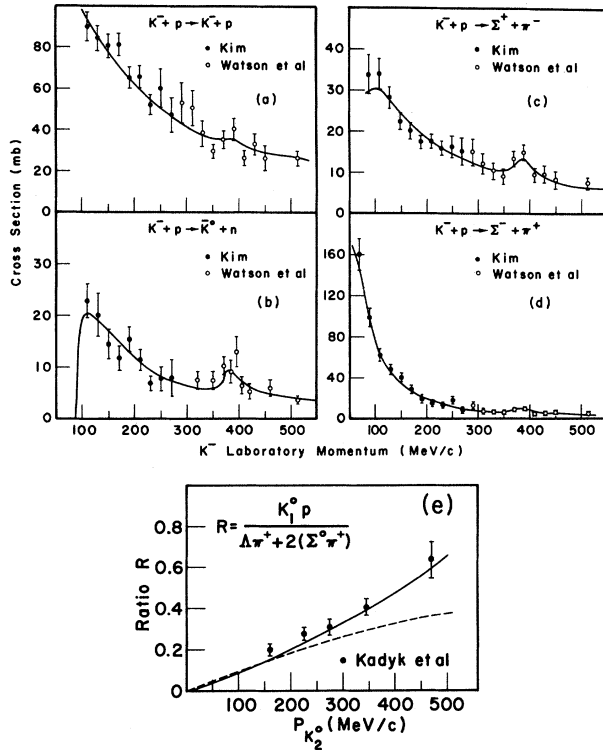


FIG. 1. (a)-(d) Total cross sections for the reactions specified. The solid curve is the expected value from the solution of Table I. (e) The solid curve is expected from the Yang set and the dashed line is from the Fermi set.

system has a pole at 1403 MeV which is caused by the factor $1 + k\alpha$. Since α is large and negative, this term can become zero at the proper energy, and it causes the pole in the $\pi\Sigma$ channel. At the pole, the $\pi\Sigma$ scattering phase goes through $\frac{1}{2}\pi$ as shown in Fig. 2(b). This type of resonance belongs to Class (b) and it is an s-wave $\bar{K}N$ virtual bound state. In order to compare this bound state with the $Y_0^*(1405)$, the $\pi\Sigma$ production cross section as a function of total center-of-mass energy according to Watson's theorem¹² is calculated and shown in Fig. 2(c) in arbitrary units. The mass and the width obtained from the effective-range parameters for this resonance are, respectively, lower and wider than the values from constant-scattering-length analyses,¹³ and these are

$$E_\gamma = 1403 \pm 3 \text{ MeV}, \quad \Gamma = 50 \pm 5 \text{ MeV}.$$

These values are in good agreement with the parameters of $Y_0^*(1405)$. The equally important agreement is in the asymmetric shape with the sharp fall on the high-mass side. Thus,

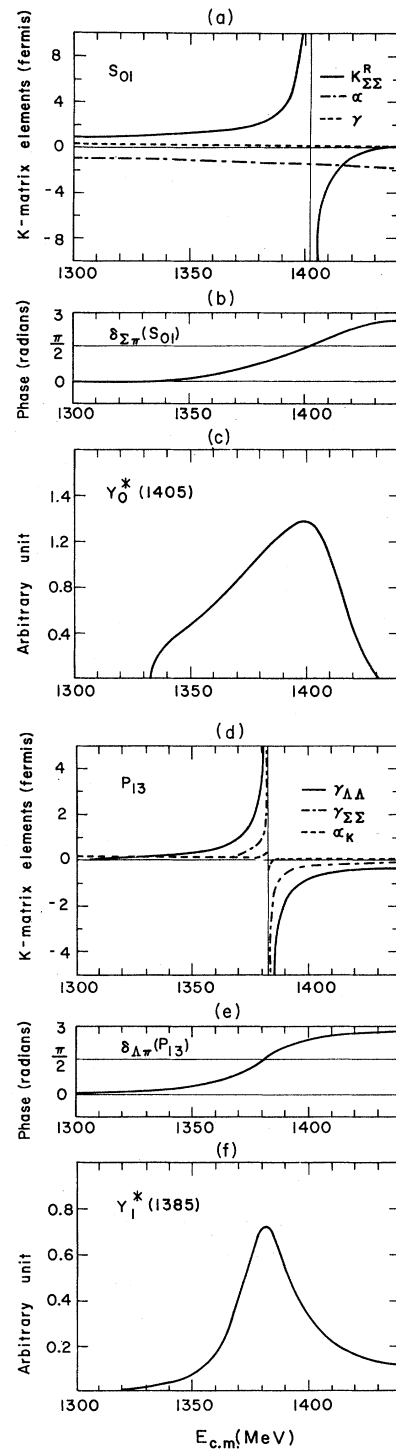


FIG. 2. (a) α and γ are the diagonal elements of the K matrix and $K_{\Sigma\Sigma}^R$ is the reduced K matrix for the $\Sigma\pi$ system for S_{01} wave. (b) $\Sigma\pi$ scattering phase shift. (c) $\Sigma\pi$ production cross section in arbitrary units for S_{01} wave. (d) α_K , $\gamma_{\Sigma\Sigma}$, and $\gamma_{\Lambda\Lambda}$ are the diagonal elements of K matrix for P_{13} wave. (e) $\Lambda\pi$ scattering eigenphase shift. (f) $\Lambda\pi$ production cross section in arbitrary units.

this analysis presents a much more comprehensive and detailed interpretation of $Y_0^*(1405)$ as an s -wave $\bar{K}N$ bound state.

The diagonal elements of the K matrix for P_{13} are shown in Fig. 2(d). All K -matrix elements have a pole at the same energy. The interaction for the $\pi\Lambda$ channel is very strong, and the $\pi\Sigma$ -channel interaction is weak. The interaction for the $\bar{K}N$ channel is negligible. Figure 2(e) shows the $\pi\Lambda$ scattering eigenphase which goes through $\frac{1}{2}\pi$ at the location of the pole. This resonance belongs to Class (a), and it can be identified with the $Y_1^*(1385)$. In the final fitting of parameters given in Table I, the location of this resonance has been fitted to 1382 MeV, as the present data do not allow the exact prediction of this mass, mainly because of statistical limitations. The $\pi\Lambda$ production cross sections calculated from Watson's theorem and the parameters of Table I are shown in Fig. 2(f). The width shown is 32 MeV, which is in good agreement with the $Y_1^*(1385)$. The symmetric shape of the resonance is also in agreement with the production data of $Y_1^*(1385)$. Therefore, $Y_1^*(1385)$ is mainly a $\pi\Lambda$ scattering resonance, and its coupling to the $\bar{K}N$ channel is very weak. It is definitely not a p -wave $\bar{K}N$ bound state.

This work was conceived and initiated while the author was at Columbia University. The author wishes to thank Professor J. Steinberger for his encouragement. It is a great pleasure to thank both Professor J. Sandweiss and Professor H. Taft for their support and encouragement during the course of this work. The author also thanks Dr. J. Kadyk for the data made available to him before publication. The search of parameters took 100 h of CDC 6600 time, and the cooperation of the New York University computing staff is greatly appreciated.

Part of this paper was written at Lawrence Radiation Laboratory, and the hospitality of Professor G. Goldhaber is appreciated.

*Work supported by the U. S. Atomic Energy Commission and National Science Foundation.

†Present address: Department of Physics, Harvard University, Cambridge, Massachusetts.

¹Preliminary results of this analysis were reported in Bull. Am. Phys. Soc. 12, 506 (1967).

²M. Ross and G. Shaw, Ann. Phys. (N.Y.) 13, 147 (1961).

³V. J. Stenger, W. E. Slater, D. H. Stork, H. K. Ticho, G. Goldhaber, and S. Goldhaber, Phys. Rev. 134, B1111 (1964).

⁴J. K. Kim, Phys. Rev. Letters 14, 29 (1965); Columbia University Report No. NEVIS-149, 1966 (unpublished).

⁵M. B. Watson, M. Ferro-Luzzi, and R. D. Tripp, Phys. Rev. 131, 2248 (1963).

⁶J. A. Kadyk, Y. Oren, G. Goldhaber, S. Goldhaber, and G. H. Trilling, Phys. Rev. Letters 17, 599 (1966); in Proceedings of the Thirteenth International Conference on High Energy Physics, Berkeley, 1966 (University of California Press, Berkeley, California, 1967), p. 203.

⁷R. Dalitz and S. Tuan, Ann. Phys. (N.Y.) 10, 307 (1960).

⁸The following momentum dependence for the resonance width has been used: $\Gamma \propto [k^2/(X^2+k^2)]^l k$, where k is the center-of-mass momentum and X is the inverse of interaction radius. See S. L. Glashow and A. H. Rosenfeld, Phys. Rev. Letters 10, 192 (1963).

⁹See A. H. Rosenfeld and W. E. Humphrey, Ann. Rev. Nucl. Sci. 13, 103 (1963).

¹⁰R. Dalitz, Rev. Mod. Phys. 33, 471 (1961).

¹¹The α , β , and γ are, respectively, $\langle \bar{K}N | K | \bar{K}N \rangle$, $\langle \bar{K}N | K | \pi Y \rangle$, and $\langle \pi Y | K | \pi Y \rangle$.

¹²K. M. Watson, Phys. Rev. 88, 1163 (1952).

¹³See Kim, Ref. 4; M. Sakitt, T. B. Day, R. G. Glasser, N. Seeman, J. Friedman, W. E. Humphrey, and R. R. Ross, Phys. Rev. 139, B719 (1965). The constant-scattering-length analyses give, respectively, $E_\gamma = 1411$, $\Gamma = 37$ by Kim and $E_\gamma = 1410$, $\Gamma = 28$ by Sakitt et al.